TELKOMNIKA Telecommunication, Computing, Electronics and Control
Vol. 19, No. 6, December 2021, pp. 2000~2008
ISSN: 1693-6930, accredited First Grade by Kemenristekdikti, Decree No: 21/E/KPT/2018
DOI: 10.12928/TELKOMNIKA.v19i6.20362

Partial discharge measurements for investigating defected solid dielectrics

Ahmed S. Haiba[1], Adel A. El-Faraskoury[2], Ahmed D. El-Koshairy[3], Mamdouh M. Halawa[4]
[1,3]Department of Electrical Engineering, Faculty of Engineering, Ain Shams University, Cairo, Egypt
[2]Extra High Voltage Research Center, Cairo, Egypt
[1,4]Department of Electrical Metrology, National Institute of Standards (NIS), Giza, Egypt

Article Info

Article history:

Received Mar 18, 2021
Revised Aug 13, 2021
Accepted Aug 21, 2021

Keywords:

Cavity
COMSOL Multiphysics
Modelling
Partial discharge measurement
Solid dielectrics

ABSTRACT

Insulation system in high voltage power equipment plays an important role for the reliability of the electric power system. So, it is necessary to assess its performance to prevent any sudden interruption in the power system. Partial discharge (PD) in solid dielectrics could occur due to the presence of a cavity or a crack within the insulating material which could be formed during manufacturing, installing or/and operating conditions. Since internal cavities are the main source of the PD activities, they can lead to causing deterioration of the insulation system and consequently a complete failure may be occurred. In this paper, PD measurement and simulation are performed on a rubber insulating material with variable cylindrical cavity diameters. High-frequency current transformer (HFCT) technique is introduced for PD measurement. Therefore, a PD simulation model is developed using COMSOL Multiphysics program interlinked with Matlab software in order to investigate the influence of cavity geometry on the PD behavior in insulating material. Both measured and simulated results indicate that PD magnitude is strongly depending on changing the cavity size inside the insulating material. The results show a good agreement between experimental and simulated data outputs in terms of maximum PD magnitude.

Corresponding Author:

Ahmed S. Haiba
Department of Electrical Metrology
National Institute of Standards (NIS)
Tersa Street, El-Haram, Giza, Egypt
Email: eng_haiba@yahoo.com, ahmedhaiba10@gmail.com

1. INTRODUCTION

Partial discharge (PD) is an internal or external electric spark occurrence that does not pass the distance among electrodes inside an electrical insulating material during electric field strength [1]. PD usually happens due to several defects such as internal small voids, cavities, or cracks inside the insulating material formed during the manufacturing process or during the operating service under electrical stress for a long term. Under operating conditions, the electric field inside the gaseous cavities exceeds the field of the insulating material and this returns to the higher permittivity of that dielectric material [2]. PD may occur if the electric field of the gaseous air in the void is enough to be large and the strength of the gas inside the void is increased [2]-[4]. During PD occurrence, the gas-filled cavity converts its insulation property to a conducted material causing decreasing the electric field inside the cavity to a lower value in a very small duration of time [5]. Since internal voids or cavities are the main sources of PD events, insulation degradation in the system

could be happened and hence, a complete failure may be occurred [6]. As a result, monitoring of PD activities is very significant tool for evaluating the performance of the insulating system.

Several experimental detection methods have been used on the basis of both electrical and non-electrical techniques for detection, analyzing, and estimation of PD activities in solid dielectrics as described in [7]-[13]. On the other hand, there are PD models that have been introduced to study the PD performance inside cavities in insulating materials. The abc-model is a traditional model that was used for modeling and simulation of PD mechanism in solid dielectrics. In this model, the insulating material and the cavity are represented as capacitors [8]. Although this model has been used to clarify some observed experimental data, it is not realistic in describing the cavity discharge process [14], [15]. Recently, with emerging modern technology and upgrading of PD software models, finite element analysis (FEA) software programs has been developed to simulate the PD behavior inside the dielectric materials and to understand the PD phenomena more deeply. This advanced tool is widely used for modeling of PD based on the geometry and the size of the cavity in solid dielectrics [1], [2], [6], [14], [16]-[19]. The model introduced in [6] studied the PD events within a spherical cavity at variable applied voltages and frequencies and the simulated results were compared to the experimental data. In addition, the model developed in [1] studied the PD behavior on a cylindrical cavity within polycarbonate plates. However, there is a shortage of usage of this advanced model on some applications such as outdoor insulators due to their complicated geometry as some researchers have studied only the distribution of potential and electric field on high voltage outdoor insulators [20], [21].

In this work, an experimental study of PD detection and measurement is carried out on a rubber solid dielectric material with variable artificial cylindrical cavity diameters. Also, COMSOL Multiphysics is used as a FEA tool which is interfaced with MATLAB program software to simulate and model the PD events resulting from the cavities inside the rubber insulating material. In addition to that, a comparison study is introduced between the measured and simulated results.

2. EXPERIMENTAL SETUP AND RESULTS

2.1. Test specimen

The samples under test were prepared with 5 cm diameter and 5 mm thickness. In order to obtain PD sources in the test samples, artificial cylindrical cavities were introduced in the rubber samples with variable diameters as 2 mm, 4 mm, 6 mm, and 8 mm in addition to the healthy one. To create the test object, three samples are used to be compressed together between two electrodes; the first one is connected to the upper cylindrical electrode, the second one is connected to the lower cylindrical electrode, and the third one containing the cavity is placed between the two other samples as shown in Figure 1. The upper and lower electrodes are cast in epoxy to prevent any discharges between electrodes and the samples. So, the test object which contains the three samples represents a rubber insulating material with an internal void or cavity. During the test, the test object with electrodes are placed in a polymer holder to be compressed together and to avoid any separations between the samples.

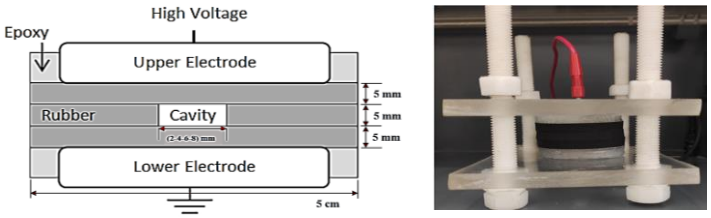

(a) (b)

Figure 1. Test object with cylindrical cavity: (a) schematic diagram of PD model and (b) experimental test object

2.2. Test setup

A high voltage dielectric test set with 100 kV step up transformer, 50 Hz, (phenix technologies) is used as AC source for applying voltage on the test object. The higher electrode is interlinked to the high voltage terminal of the transformer and the lower one is grounded. PD is detected by High-frequency current transformer (HFCT) (CT100) which is placed around the ground terminal and connected to MPD540 acquisition unit which is connected to a battery. A fibre optical cable is used to connect the MPD540 unit to the USB502 then to a personal computer as shown in Figure 2.

An alternating current (AC) voltage, 50 Hz, is applied to the test object to produce PD activities resulting from artificial cavities. HFCT operation depends on the detection of current pulses with high

frequency that could be happened during PD in the test object. These current pulses are converted into charges which usually expressed in pico coulombs (pC) [22], [23].

2.3. Results

According to the schematic diagram shown in Figure 2, the apparent charge is measured for each cavity diameter in addition to the healthy sample at laboratory ambient conditions. Before performing the test, PD measuring system shall be calibrated by a reference PD calibrator (LDC-5/R) as recommended in IEC standards and corresponding researches [22], [24]. Figure 3 shows the example of PD level measurements pattern with artificial cavities for diameter 4- and 8-mm. Apparent charge is measured with different applied voltages for each test object as shown in Figure 4. It has been seen that the PD magnitude increases with increasing both applied voltage and the cavity diameter. The charge value of the sample without cavity is the lowest value and the sample with 8 mm cavity diameter is the highest value. Also, it has been observed from this experiment that the inception voltage is noticed to be around 5.45 kV, 5.23 kV, 5.01 kV, and 4.82 kV for cavity diameters 2, 4, 6 and 8 mm respectively.

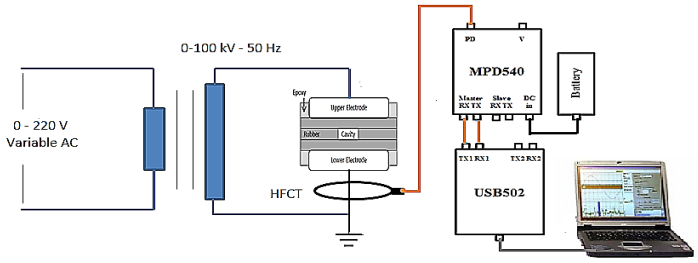

Figure 2. Experimental test setup for PD measurement system

(a)

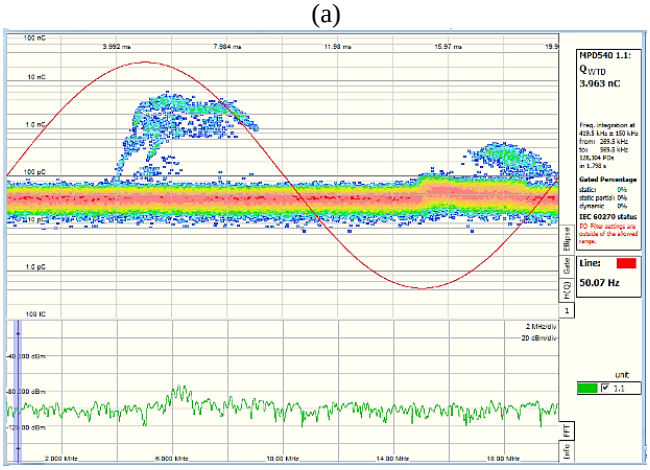

(b)

Figure 3. Example of PD measurements pattern at 30 kV, for: (a) 4 mm and (b) 8 mm

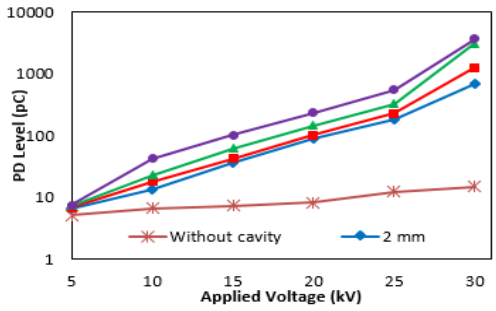

Figure 4. PD magnitude at variable applied voltages for all samples

3. PD MODEL SIMULATION

In this study, a PD model is developed using COMSOL Multiphysics software as a FEA tool which interfaced with MATLAB software. The geometry of the model is carried out in two dimensional (2D) axial symmetric depending on the unit under test that was used in the measurement section with different cavity diameters. The model consists of four main parts; a homogenous insulation material (rubber), a cylindrical cavity with 2, 4, 6 and 8 mm diameters, a cavity surface of 0.1 mm thickness, and two copper electrodes as shown in Figure 5.

After adding the data for all used materials from COMSOL library or by manual, boundaries for each section are created. The upper copper electrode is set as boundary potential ($V= V_{app.} \sin(100\pi t)$) and the lower electrode is set as boundary ground ($V = 0$). After that, the meshes in the model are refined to obtain more accurate results [2].

In this model, it is assumed that the insulation material (rubber) is homogeneous and the PD events occur at the cavity center due to the strongest concentration of the electric field in the cavity center [2], [16]. The electric potential and electric field distributions through the developed model are solved by (1) [1], [16], [19] by choosing 'electric current (ec)' from 'AC/DC module'. For sinusoidal applied voltage, time dependent study is selected to be used for solver settings.

$$\nabla \cdot \left[-\sigma \nabla V - \frac{\partial}{\partial t}(\varepsilon_o \varepsilon_r \nabla V)\right] = 0 \quad (1)$$

Where: V is the electric voltage, σ is the conductivity, ε_o is the vacuum permittivity, and ε_r is the relative permittivity.

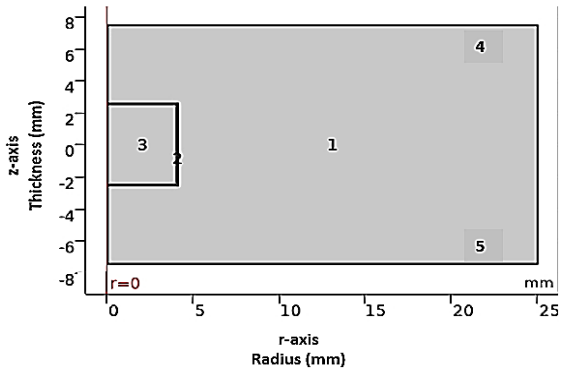

Figure 5. 2D geometry of the model in COMSOL program
(1: insulation material, 2: cavity surface, 3: cavity, 4: potential electrode, 5: grounded electrode)

3.1. PD occurrence

In this model, two necessary conditions are required for PD occurrence in a cavity [1], [2], [14], [16], [17], [19], [25]; the first condition is the electric voltage in the void shall be greater than the intensity of the breakdown of the gas which corresponds to the cavity inception voltage (V_{inc}), and the second condition is that free electrons must be available enough inside the cavity to start an electron avalanche process. So, the first condition can be achieved by testing that the cavity voltage (V_{cav}) is greater than the voltage inception (V_{inc})

that required to initiate PD event. For the second condition, free electrons in the cavity in this study are obtained only from cavity surface emission as in [1], [16] depending on the electron generation rate (N_e) according to (2) [1], [16], [19].

$$N_e(t) = N_{e0}\exp(|V_{cav}(t)/V_{inc}(t)|) \quad (2)$$

Where: V_{cav} is the voltage through the cavity center, V_{inc} is the inception voltage to initiate PD event, and N_{e0} is a constant.

In (2) is very simple for electron generation rate based on Ritchardson-Schottky law [19], [26]. Sometimes the number of free electrons is poor for starting electron avalanche. So, the electron generation rate and PD occurrence are considered as a stochastic process [1]. Consequently, the probability (P) of generating a free electron in the cavity in a time step (dt) is assumed to be $N_e(t)dt$ according to (3) [1], [16], [19]. Then the acquired probability value is compared with a random number (R) which has a uniform distribution from 0 to 1 ($0 < R < 1$). At each time step there is a possibility of PD occurrence if $V_{cav} > V_{inc}$ and $P > R$.

$$P = N_e(t) \quad (3)$$

Since the time of the discharge is very short almost in a little nanosecond, the electric potential in the cavity drops sharply within a short time period [16]. After a PD event, the electric potential inside the cavity is decreased causing the released electrons to lose their accelerated energy and the conductivity and the current decrease inside the cavity. When the electric voltage inside the cavity reduced to become lower than the voltage extinction (V_{ext}), the PD activity stopped [2].

In this current study, PD activity inside the void is modeled dynamically with increasing the conductivity of the cylindrical cavity according to (4) [1], [19].

$$\sigma_{cav} = \begin{cases} \sigma_0 \boldsymbol{e}^{\left(\left|\frac{V_{cav}}{V_{inc}}\right| + \left|\frac{I_{cav}}{I_0}\right|\right)} & during\ discharge \\ \sigma_0 & no\ discharge \end{cases} \quad (4)$$

Where: σ_0 is the initial cavity conductivity at no discharge, I_{cav} is the current through the void, and I_0 is the initiation current at an electron avalanche onset

The current in the cavity during discharge can be calculated according to (5) [1], [19].

$$I_{cav} = \begin{cases} \iint \boldsymbol{J}.\boldsymbol{ds} & during\ discharge \\ 0 & no\ discharge \end{cases} \quad (5)$$

Where: $\boldsymbol{J}$ is the current density through the cavity. Finally, the physical charge value (q) due to PD event is calculated according to (6) [2], [19].

$$q = \int_t^{t+dt} I_{cav}(t)\, dt \quad (6)$$

4. SIMULATION RESULTS AND DISCUSSION

The parameters that used in this model are assumed as shown and described in Table 1 represented in a MATLAB interactive menu at the beginning run of the model. The inception voltage (V_{inc}), the extinction voltage (V_{ext}), and the initial electron generation rate (N_{e0}) are selected to be compatible with the measured results at 50 Hz. Figures 6(a) and 6(b) show the distribution of the electric potential and electric field in the rubber material and the cavity in case of 8 mm diameter, for example, before the occurrence of PD in the cavity respectively. It has been observed from Figure 6(b) that the electric field inside the cavity is larger than that in the surrounding rubber material because of the higher dielectric constant of the rubber material. Therefore, the electric field on the top and bottom of the surface wall of the cavity nearest to the electrodes is low because the applied electric field is perpendicular to the surface of the cavity [2].

Furthermore, Figure 7(a) shows the electric potential after PD occurrence. Also, Figure 7(b) shows the electric field distribution after PD event. It has been observed from Figure 7(b) that the electric field across the cavity seems to be less than that of the surrounding rubber material because of the dynamic motion of electrons inside the cavity [2]. In addition, the electric field on the top and bottom of the cavity surface closest to the electrodes is high. After PD occurrence, charges accumulate on the surface wall of the cavity producing an opposite electric field which decreases the electric field inside the cavity [2].

Table 1. Definition of used parameters in the model

Symbol	Value	Description
V_{app}	30 kV	Test voltage
f	50 Hz	Rated frequency
V_{ext}	2 kV	Extinction voltage
E_{mat}	4	Permittivity of rubber material
E_{rcav}	1	Cavity permittivity
E_{rs}	4	Cavity surface permittivity
E_{cu}	1	Copper permittivity
S_{mat}	1×10^{-13} S/m	Rubber conductivity
S_{cav}	1×10^{-15} S/m	Cavity conductivity
S_s	1×10^{-13} S/m	Cavity surface conductivity
S_{cu}	5.813×10^{7} S/m	Copper conductivity
S_{cavmax}	1×10^{-4} S/m	Max. conductivity of cavity
N_{e0}	650 1/s	Initial electron generation rate
I_0	1×10^{-10} A	Initiating current at an electron avalanche onset

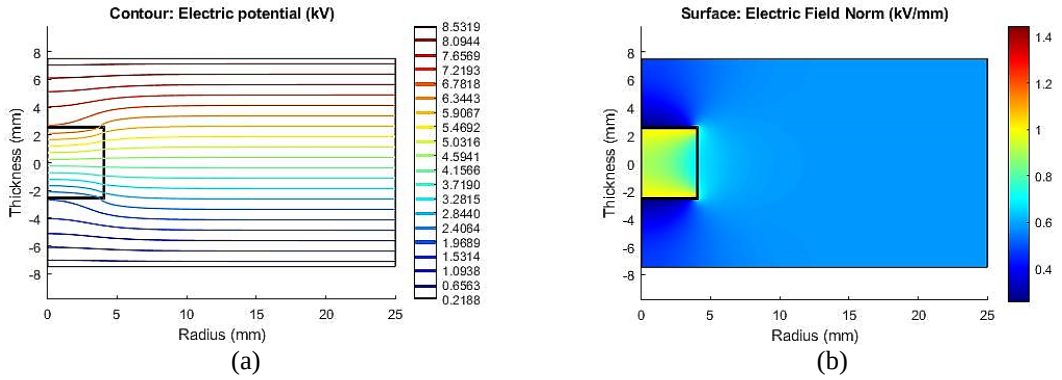

(a) (b)

Figure 6. Distributions before the PD event, for (a) Electric potential and (b) Electric field

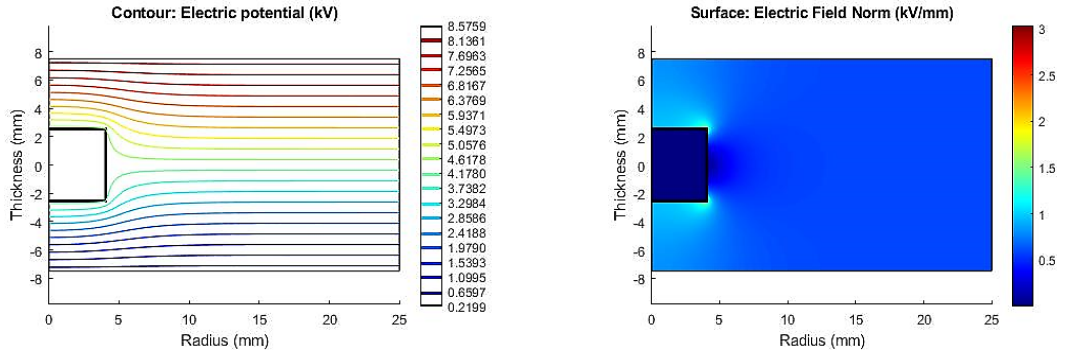

(a) (b)

Figure 7. Distributions after the PD event, for (a) Electric potential and (b) Electric field

Figures 8-11 show the simulation of V_{app}, V_{cav}, V_{inc}, V_{ext}, and charge magnitude against the phase angle during one cycle for 2 mm, 4 mm, 6 mm, and 8 mm cavity diameters. Initially, the cavity voltage starts from zero with the applied voltage, and then it exceeds as the applied voltage increases. When the cavity voltage arrives to the inception voltage and more released electrons are available radiated from the surface of the cavity, the PD can occur. Immediately after PD occurrence, the cavity voltage drops sharply until reaching to the extinction voltage where the discharge stops. Increasing the cavity conductivity causes the voltage inside the cavity again to be increased and the discharges repeated. It has been seen from these figures that, PD occurs immediately when the cavity voltage reaches to the inception voltage due to the availability of free electrons for a PD to occur. This process is repeated in the two half cycles of the applied voltage and continues untill stopping the applied voltage. Therefore, increasing the cavity diameter increases the PD repetition rates of occurrence and increases the maximum PD magnitude. Also, it has been observed that with increasing cavity diameter, PD occurs at earlier time and this returns to the availability of electrons from the cavity surface at earlier time.

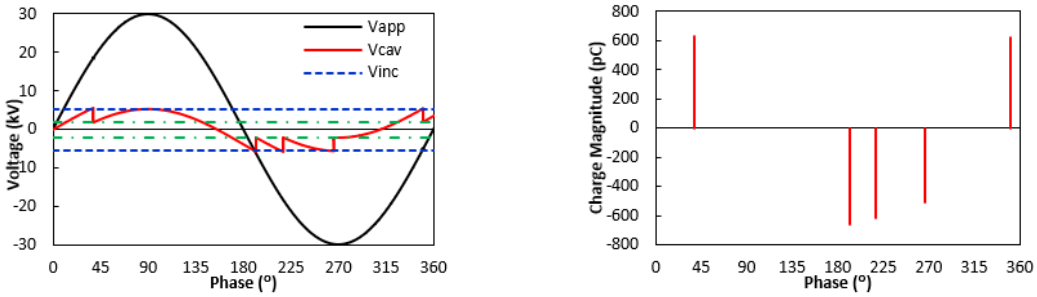

Figure 8. Voltage at cavity and PD magnitude with phase angle for one-cycle at 2 mm cavity diameter

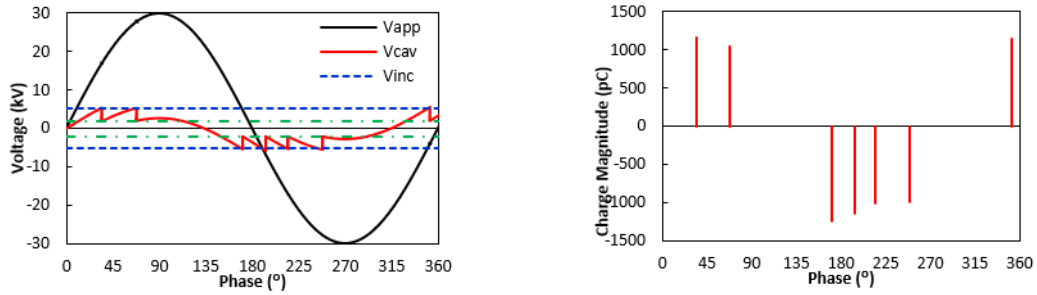

Figure 9. Voltage at cavity and PD magnitude with phase angle for one-cycle at 4 mm cavity diameter

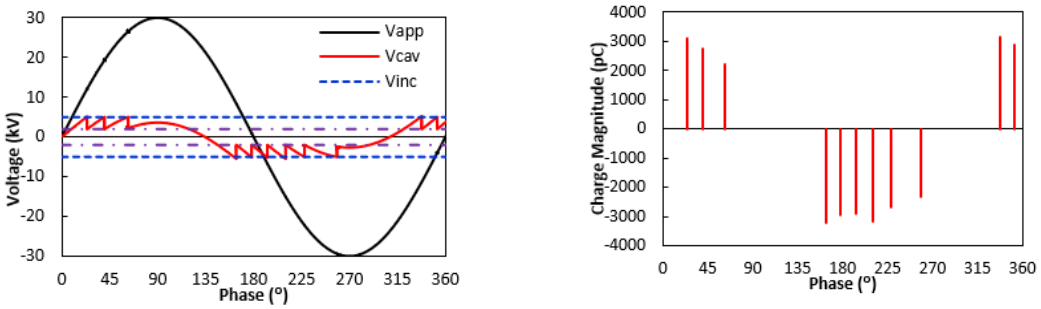

Figure 10. Voltage at cavity and PD magnitude with phase angle for one-cycle at 6 mm cavity

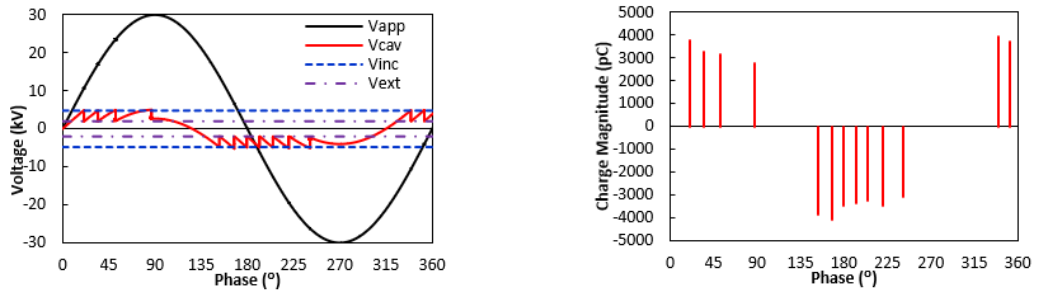

Figure 11. Voltage at cavity and PD magnitude with phase angle for one-cycle at 8 mm cavity diameter

5. COMPARISON BETWEEN MEASURED AND SIMULATED RESULTS

Table 2 summarizes the measured and simulated results obtained at 30 kV applied voltage, 50 Hz. The comparison is based on the maximum PD magnitude in all cavity diameters. It has clearly indicated from Table 2 and Figure 12 that the results obtained from simulation model are compatible, to a great extent, with those acquired from the experimental measurement for the four studied cavity diameters with a maximum error of 8.20 %.

Table 2. Measured and simulated results for all cavity diameters

Cavity diameter (mm)	Maximum PD measured (pC)	Maximum PD simulated (pC)	Error ± (%)
2	717.4	658.6	8.20
4	1295	1236	4.56
6	3163	3213	1.58
8	3984	4074	2.26

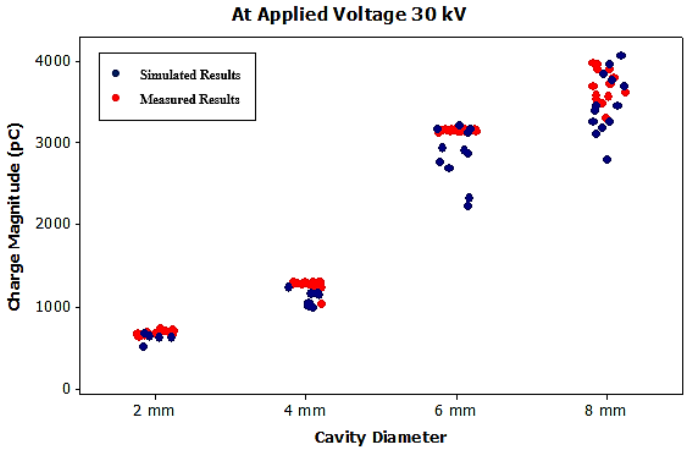

Figure 12. Experimental and simulation results at 30 kV and 50 Hz

6. CONCLUSION

In this current work, PD measurement and simulation were performed on a rubber sample with an artificial variable cavity diameter to discuss the influence of cavity diameter on the behavior of PD activities. PD measurement was carried out by using HFCT technique indicating that the PD magnitude is strongly depending on the spatial geometry of the cavity inside the insulating material as well as increasing the cavity diameter increases the PD magnitude depending on the applied voltage. Also, a PD simulated model is developed using COMSOL Multiphysics interfaced with MATLAB software for extending a deeper understanding of PD occurrence inside a cavity. The simulated model studies the distribution of the electric potential and electric field inside the cavity in case of before and after occurrence of PD. Therefore, simulation results indicate the PD magnitude and PD repetition rate increase with increasing cavity diameters and PD occurs at earlier time for large cavity diameter due to the availability of free electrons emitted from the cavity surface at earlier time. The results acquired from the simulation model matches with those obtained from the experimental study with a maximum error of 8.20 % based on the maximum PD magnitudes at 30 kV and 50 Hz.

ACKNOWLEDGEMENTS

The authors would like to express their deep thanks to the experts in National Institute of Standards (NIS), Giza, Egypt, for their help in samples preparation. Also, the authors are grateful to El-Nasr Transformers and Electrical Products-El-MACO Company for helping in testing and measurements.

REFERENCES

[1] G. Chen and F. Baharudin, "Partial discharge modelling based on a cylindrical model in solid dielectrics," *2008 International Conference on Condition Monitoring and Diagnosis*, 2008, pp. 74-78, doi: 10.1109/CMD.2008.4580233.

[2] H. A. Illias, "Measurement and simulation of partial discharges within a spherical cavity in a solid dielectric material," PhD Thesis, University of Southampton, May 2011.

[3] E. Kuffel, W. Zaengl, and J. Kuffel, "High voltage engineering fundamentals," Book, 2nd edition, Newnes: Butterworth-Heinemann, 2000.

[4] S. A. Boggs, "Partial discharge. III. Cavity-induced PD in solid dielectrics," *IEEE Electrical Insulation Magazine*, vol. 6, no. 6, pp. 11-16, Nov.-Dec. 1990, doi: 10.1109/57.63094.

[5] S. Boggs and J. Densley, "Fundamentals of partial discharge in the context of field cable testing," in *IEEE Electrical Insulation Magazine*, vol. 16, no. 5, pp. 13-18, Sept.-Oct. 2000, doi: 10.1109/57.871416.

[6] H. Illias, G. Chen, and P. L. Lewin, "Partial discharge behavior within a spherical cavity in a solid dielectric material as a function of frequency and amplitude of the applied voltage," in *IEEE Transactions on Dielectrics and Electrical Insulation*, vol. 18, no. 2, pp. 432-443, April 2011, doi: 10.1109/TDEI.2011.5739447.
[7] A. S. Haiba, A. Gad, S. M. Eldebeikey, and M. Halawa, "Statistical Significance of Wavelet Extracted Features in the Condition Monitoring of Ceramic Outdoor Insulators," in *IEEE Electrical Insulation Conference (EIC)*, 2019, pp. 432-435, doi: 10.1109/EIC43217.2019.9046590.
[8] M. Albano, R. T. Waters, P. Charalampidis, H. Griffiths, and A. Haddad, "Infrared analysis of dry-band flashover of silicone rubber insulators," in *IEEE Transactions on Dielectrics and Electrical Insulation*, vol. 23, no. 1, pp. 304-310, February 2016, doi: 10.1109/TDEI.2015.005026.
[9] F. Paweł, U. Ireneusz, and F. Joachim, "Comparison of two methods for detection of UV signals emitted by PD on HV insulators made of porcelain," *PRZEGLĄD ELEKTROTECHNICZNY*, vol. 92, pp. 102-104, August 2016, doi: 10.15199/48.2016.08.28.
[10] W. R. Si, J. H. Li, D. J. Li, J. G. Yang, and Y. M. Li, "Investigation of a comprehensive identification method used in acoustic detection system for GIS," in *IEEE Transactions on Dielectrics and Electrical Insulation*, vol. 17, no. 3, pp. 721-732, June 2010, doi: 10.1109/TDEI.2010.5492244.
[11] M. M. Yaacob, M. A. Alsaedi, J. R. Rashed, A. M. Dakhil, and S. F. Atyah, "Review on partial discharge detection techniques related to high voltage power equipment using different sensors," *Photonic Sensors*, vol. 4, no. 4, pp. 325–337, 2014, doi: 10.1007/s13320-014-0146-7.
[12] C. Min, K. Urano, L. Y.-Cheng, and A. Jinno, "Application of combined PD sensor for GIS PD detection and condition monitoring," in *2008 International Conference on Condition Monitoring and Diagnosis*, 2008, pp. 456-460, doi: 10.1109/CMD.2008.4580324.
[13] M. D. Judd, L. Yang, and I. B. B. Hunter, "Partial discharge monitoring of power transformers using UHF sensors. Part I: sensors and signal interpretation," in *IEEE Electrical Insulation Magazine*, vol. 21, no. 2, pp. 5-14, March-April 2005, doi: 10.1109/MEI.2005.1412214.
[14] M. Borghei and M. Ghassemi, "Finite Element Modeling of Partial Discharge Activity within a Spherical Cavity in a Solid Dielectric Material under Fast, Repetitive Voltage Pulses," in *IEEE Electrical Insulation Conference (EIC)*, 2019, pp. 34-37, doi: 10.1109/EIC43217.2019.9046525.
[15] G. C. Crichton, P. W. Karlsson, and A. Pedersen, "Partial discharges in ellipsoidal and spheroidal voids," in *IEEE Transactions on Electrical Insulation*, vol. 24, no. 2, pp. 335-342, April 1989, doi: 10.1109/14.90292.
[16] C. Forssen and H. Edin, "Partial discharges in a cavity at variable applied frequency part 2: measurements and modeling," in *IEEE Transactions on Dielectrics and Electrical Insulation*, vol. 15, no. 6, pp. 1610-1616, December 2008, doi: 10.1109/TDEI.2008.4712664.
[17] H. Illias, L. T. Jian, A. H. A. Bakar, and H. Mokhlis, "Partial discharge simulation under various applied voltage waveforms," *in 2012 IEEE International Conference on Power and Energy (PECon)*, 2012, pp. 967-972, doi: 10.1109/PECon.2012.6450358.
[18] H. Illias, G. Chen, and P. L. Lewin, "Modeling of partial discharge activity in spherical cavities within a dielectric material," in *IEEE Electrical Insulation Magazine*, vol. 27, no. 1, pp. 38-45, January-February 2011, doi: 10.1109/MEI.2011.5699446.
[19] O. E. Gouda, A. A. El-Farskoury, A. R. Elsinnary, and A. A. Farag, "Investigating the effect of cavity size within medium-voltage power cable on partial discharge behavior," *IET Generation, Transmission & Distribution*, vol. 12, no. 5, pp. 1190-1197, 2018, doi: 10.1049/iet-gtd.2017.1012.
[20] Z. Ali, M. Ali, S. Khokhar, N. Ahmed, and M. Ali, "Modeling of high voltage insulator strings through finite element method," *International Journal of Computer Science and Network Security (IJCSNS)*, vol. 18, no. 8, pp. 65-69, Aug. 2018. [Online]. Available: http://paper.ijcsns.org/07_book/201808/20180809.pdf
[21] H. Benguesmia, N. M'ziou, and A. Boubakaur, "Simulation of the potential and electric field distribution on high voltage insulator using the finite element method," *Diagnostyka*, vol. 19, no. 2, pp. 41-52, 2018, doi: 10.29354/diag/86414.
[22] IEC 60270, *High Voltage Testing-Partial Discharge Measurement: The European Standard EN 60270:2001 has the status of a British Standard*, British Standard 2000. [Online]. Available: https://teslapishro.ir/wp-content/uploads/2019/12/High-voltage-test-technique.pdf
[23] IEC 62478, *High voltage test techniques-Measurement of partial discharges by electromagnetic and acoustic methods*, 1st ed., BSI Standards Publication, 2016.
[24] A. El-Faraskoury, M. Mokhtar, M. Mehanna, and O. Gouda, "Experience of Partial Discharge with IEC Type Testing and after Installation Testing for extruded Cables," in *CIGRE Conference*, Paris, August 2014, doi: 10.13140/2.1.1851.7285.
[25] A. Patil, D. Patil, R. Pangarkar, and D. Patil, "Modelling and FEA Analysis of Partial Discharge Phenomena in a Spherical Void within Solid Dielectric Material," in *2018 International Conference on Current Trends towards Converging Technologies (ICCTCT)*, 2018, pp. 1-4, doi: 10.1109/ICCTCT.2018.8550930.
[26] L. Niemeyer, "A generalized approach to partial discharge modeling," *IEEE Transactions on Dielectrics and Electrical Insulation*, vol. 2, no. 4, pp. 510-528, Aug. 1995, doi: 10.1109/94.407017.